College of Earth and Mineral Sciences

PENNSTATE

DEPARTMENT OF MATERIALS SCIENCE

METALLURGY PROGRAM

TECHNICAL REPORT

October 1988

OFFICE OF NAVAL RESEARCH

Contract No. N00014-84-k-0201

A MECHANISTIC ANALYSIS OF HYDROGEN ENTRY INTO METALS DURING CATHODIC HYDROGEN CHARGING

Howard W. Pickering

Department of Materials Science and Engineering
The Pennsylvania State University

SECURITY CLASSIFICATION OF THIS PAGE (When Data Entered)

REPORT DOCUMENTATION PAGE		READ INSTRUCTIONS BEFORE COMPLETING FORM
1. REPORT NUMBER	2. GOVT ACCESSION NO. AD-A200747	3. RECIPIENT'S CATALOG NUMBER
4. TITLE (and Subtitle) A Mechanistic Analysis of Hydrogen Entry Into Metals During Cathodic Hydrogen Charging		5. TYPE OF REPORT & PERIOD COVERED Technical Report 6. PERFORMING ORG. REPORT NUMBER
7. AUTHOR(s) Howard W. Pickering		8. CONTRACT OR GRANT NUMBER(s) N00014-84-k-0201
9. PERFORMING ORGANIZATION NAME AND ADDRESS The Pennsylvania State University		10. PROGRAM ELEMENT, PROJECT, TASK AREA & WORK UNIT NUMBERS
11. CONTROLLING OFFICE NAME AND ADDRESS		12. REPORT DATE October 1988 13. NUMBER OF PAGES
14. MONITORING AGENCY NAME & ADDRESS(if different from Controlling Office)		15. SECURITY CLASS. (of this report) 15a. DECLASSIFICATION/DOWNGRADING SCHEDULE
16. DISTRIBUTION STATEMENT (of this Report)		
17. DISTRIBUTION STATEMENT (of the abstract entered in Block 20, if different from Report)		
18. SUPPLEMENTARY NOTES		
19. KEY WORDS (Continue on reverse side if necessary and identify by block number)		

20. ABSTRACT (Continue on reverse side if necessary and identify by block number)

The present paper seeks to analyze the h.e.r. mechanism and to predict the relationship between the permeation flux and the charging and evolution (recombination) fluxes. A thorough development of the model and actual computations of rate constants and hydrogen coverages will appear elsewhere.

DD FORM 1 JAN 73 1473 EDITION OF 1 NOV 65 IS OBSOLETE
S/N 0102-LF-014-6601

SECURITY CLASSIFICATION OF THIS PAGE (When Data Entered)

Scripta METALLURGICA Vol. 22, pp. 911-916, 1988
Printed in the U.S.A.

A MECHANISTIC ANALYSIS OF HYDROGEN ENTRY INTO METALS DURING CATHODIC HYDROGEN CHARGING

Rajan N. Iyer and Howard W. Pickering
Department of Materials Science and Engineering
The Pennsylvania State University
University Park, PA 16802
and
Mehrooz Zamanzadeh
Professional Services Industries - PTL Division
850 Poplar Street
Pittsburgh, PA 15220

(Received March 9, 1988)
(Revised April 5, 1988)

Introduction

Entry of hydrogen into metals is of serious concern to metallurgists and engineers, since it severely degrades the mechanical properties of metals (1). These problems arise in the cathodic protection of metals, power plants, and in environments where H_2S is present as in petroleum refining (2) where the hydrogen evolution reaction (h.e.r.) and hydrogen permeation reaction take place in the corroding or cathodically polarized metal. By performing hydrogen charging experiments of thin samples using the Devanathan-Stachurski cell, the permeation characteristics have been extensively studied (3,4). The present paper seeks to analyze the h.e.r. mechanism and to predict the relationship between the permeation flux and the charging and evolution (recombination) fluxes. A thorough development of the model and actual computations of rate constants and hydrogen coverages will appear elsewhere (5).

Analysis

Essentially, three steps are involved during cathodic hydrogen charging of metals. They are: (1) the hydrogen discharge reaction (proton tunneling), (2) hydrogen recombination reaction either by chemical recombination or electrochemical desorption, and (3) hydrogen permeation (mainly by bulk diffusion). Of these three, the bulk diffusion step is usually the slowest. A detailed schematic of the reactions is given in Fig. 1 below.

The charging current (i_c) is given by

$$i_c = i_o' (1 - \theta_s)\ e^{-a\alpha\eta} \qquad (1)$$

The hydrogen evolution current (i_r) (assuming chemical recombination of H atoms) is given by

$$i_r = F k_3 \theta_s^2 \qquad (2)$$

0036-9748/88 $3.00 + .00

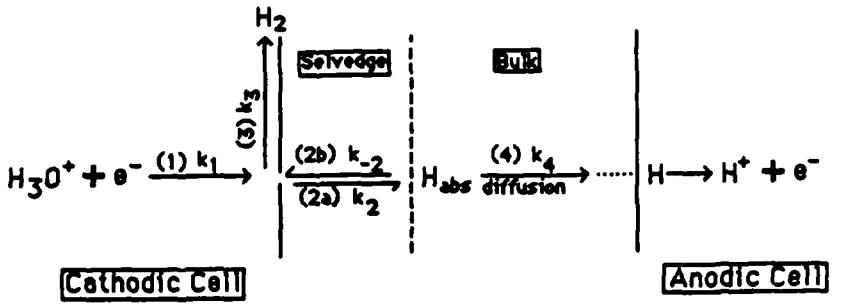

FIG. 1. Schematic showing hydrogen discharge, recombination, permeation and selvedge reactions.

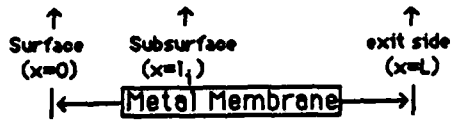

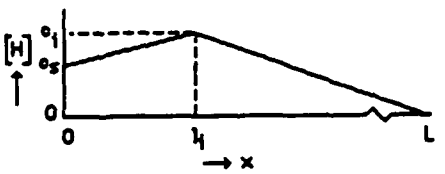

The steady state hydrogen permeation current (i_∞) is given by

$$i_\infty \equiv F\frac{D_l}{L}c_i \qquad (3)$$

In equations 1, 2 and 3: $i_o' = Fk_1 = i_o/(1-\theta_e)$; i_o = the exchange current density; θ_e = the equilibrium surface coverage of hydrogen ; k_1 = the discharge rate coefficient = $k_1^o c_{H^+} e^{-a\alpha E^{eq}}$ (acid) = $k_1^o e^{-a\alpha E^{eq}}$ (alkaline); k_1^o = the rate constant for the forward reaction; $c_{H^+} = H^+$ ion concentration; a = F/RT = 38.94 (volts)$^{-1}$ at T = 300K; α = the transfer coefficient; E^{eq} = the equilibrium potential for the h.e.r; θ_s = the surface coverage of hydrogen; η = the hydrogen overvoltage = E applied - E^{eq}; k_3 = the recombination rate coefficient; D_l = the hydrogen diffusion coefficient in the metal; L = the membrane thickness.

The model considers a selvedge reaction (as a result of proton tunneling) that is quite fast and constitutes a transition layer of a thickness that could range upward from $\sim$ 1 nm (that has yet to be determined by special experiments). This establishes a metal subsurface hydrogen concentration, c_i, at the boundary of the selvedge. Thus, hydrogen diffuses out to either surface, though mostly to the charging side to recombine to form H_2 molecules. An equilibrium will be established between the surface covered (adsorbed) hydrogen atoms and hydrogen just below the surface (in the adsorbed state, with concentration c_s). This equilibrium has been analyzed before (6,7) giving $\theta_s = c_s/k'$, where k' =

the equilibrium absorption - adsorption constant and $c_s = c_i - c_g$. (However, it is to be emphasized here that the selvedge reaction is not critical to the development and application of this model. Consideration of selvedge, on the other hand, helps to generalize the model; in the absence of a selvedge, $c_g = 0$ and $c_s = c_i$). Using these relations along with equations (1), (2) and (3) one can arrive at the following set of equations, which for the first time have taken into account the effect of i_{ss} on the h.e.r. kinetics:

$$i_{ss} = \left(\frac{k'}{b\sqrt{Fk_3}}\right)\sqrt{i_r} + \frac{c_g}{b} \qquad (4)$$

and

$$i_c e^{a\alpha\eta} = \left(\frac{bi_o'}{k'}\right)\left(i_{ss} - \frac{c_g}{b}\right) + i_o' \qquad (5)$$

where $b = L/(FD_1)$ = a constant for a metal; also,

$$\left|-120\frac{mV}{decade}\right| \sim \left|\frac{d\eta}{d\log i_c}\right| < \left|\frac{d\eta}{d\log i_{ss}}\right| < 2\left|\frac{d\eta}{d\log i_c}\right| < \left|-240\frac{mV}{decade}\right| \qquad (6)$$

for the model.

The transfer coefficient is given by

$$\alpha \equiv -\left(\frac{d\ln i_c}{d\eta}\right)/a \qquad (6a)$$

Details of the derivations are shown elsewhere (5).

The potential range (η_c^l to η_c^u) in which the recombination reaction will be coupled with the discharge reaction (commonly observed on many metals) is given by (5)

$$\eta_c^l = \left[\ln (10k_1/k_3)\right] / (a\alpha) \qquad (7a)$$

$$\eta_c^u = \left[\ln (k_1/(10k_3))\right] / (a\alpha) \qquad (7b)$$

where the superscripts l and u refer to the lower and upper limits of the overpotential range.

Results and Discussion

In hydrogen permeation experiments, i_C is set and when the permeation current becomes independent of time, i_{ss} is measured. Then $i_r = i_C - i_{ss}$.

If the plots of i_{ss} vs $\sqrt{i_r}$ (equation (4)) and $i_C\, e^{a\alpha\eta}$ vs $[i_{ss} - \frac{c_g}{b}]$ (equation (5)) are linear, then all of the coefficients k', k_3, c_g and i_o' can be calculated. Such calculations have been done on experimental data from the literature for iron and nickel membranes and found to verify the model (5) since these two plots are linear. An example of such an analysis is given for the polarization and

permeation data of Bockris et al (3) obtained on Armco iron in 0.1N H_2SO_4 solution. Fig. 2 shows the plot of i_∞ vs $\sqrt{i_r}$ and Fig. 3 shows $i_c\, e^{\alpha\eta}$ vs $[i_\infty - \frac{c_g}{b}]$ plot for the data of Bockris et al (3). It is easily seen that these plots are linear and hence the model can be applied to determine the rate constants and exchange current density (Table 1). Then, from Eqn. (2), θ_s can be calculated using the k' and i_o' values obtained from the slope and intercept, respectively, of Fig. 3, the k_3 value obtained from the slope of Fig. 2 and the i_r value from $i_c - i_\infty$. The surface coverage (θ_s) vs the hydrogen overvoltage (η) plot (for the Bockris et al data) is shown in Fig. 4. It can be seen that the coverage is quite low in the potential range of experimentation.

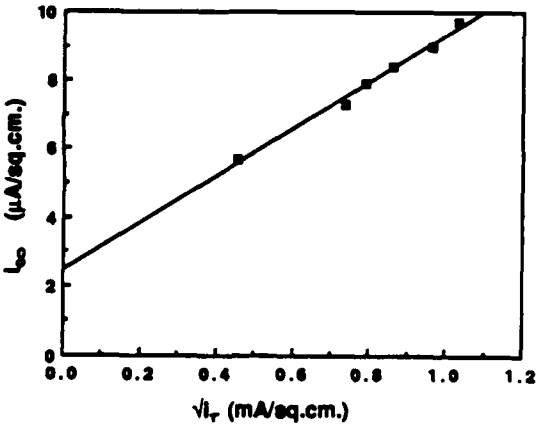

FIG. 2. Analysis of Data of Bockris et al (3).

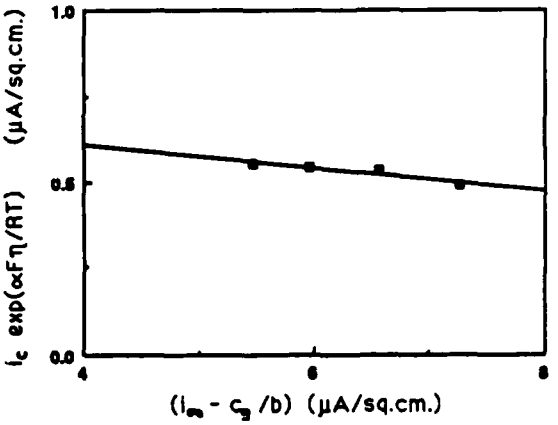

FIG. 3. Analysis of Data of Bockris et al (3).

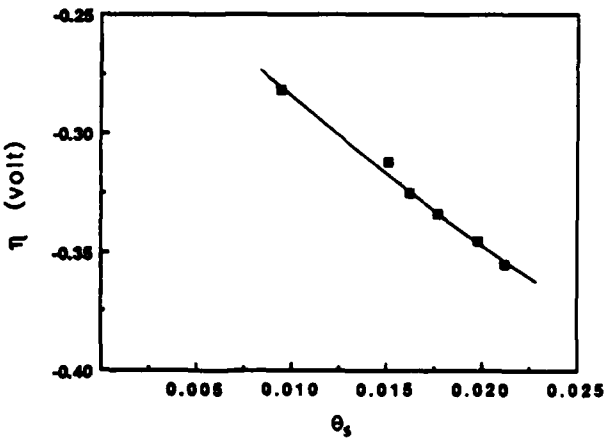

FIG. 4. H Coverage for the Data of Bockris et al (3).

TABLE 1
Calculated Values by Applying the Model to the Data of Bockris et al (3)

$i_o = 0.5$ μA/sq.cm.
$k_1 = 5.5 \times 10^{-12}$ mol / cm^2.s
$k_3 = 2.3 \times 10^{-5}$ mol /(cm^2.s
$k' = 2.6 \times 10^{-5}$ mol /cm^3
$\eta_c^l = -600$ mV ; $\eta_c^u = -810$mV

Thus, this model effectively accounts for the contribution of i_{∞} to the overall kinetics. The most important prediction of this model is that i_{∞} is proportional to $\sqrt{i_r}$ and not to $\sqrt{i_c}$ as assumed in earlier models (3). This type of relationship ($i_{\infty} \propto \sqrt{i_r}$) has been previously observed (8).

The above relationships assume that $\eta >> RT/F$ so that the backward reactions can be neglected. Also, the Langmuir isotherm of hydrogen coverage was utilized in order to simplify the derivation. However, in many cases, the reactions (discharge and recombination) are activated in which case Frumkin-Temkin corrections (9) have to be applied for θ_s in the equations for i_c and i_r. Equation (1) then becomes:

$$i_c = i_o' (1-\theta_s) e^{-\alpha f \theta_s} e^{-\alpha a \eta} \qquad (8)$$

and equation (2) becomes

$$i_r = F k_3 \theta_s^2 e^{2\alpha f \theta_s} \qquad (9)$$

where $f = \gamma/RT$, γ being the gradient of the apparent standard free energy of adsorption with coverage. The value of $f = 4$ to 5 for H coverages (9). In the problem of enhanced hydrogen entry in the presence of H_2S, such considerations have been shown to be necessary (10). The modified relationships between i_{∞}, i_r and i_c are given by

$$\ln\left(\frac{\sqrt{i_r}}{i_{\infty}}\right) = \left(\frac{\alpha f b}{k'}\right) i_{\infty} - \ln\left(\frac{k'}{b\sqrt{Fk_3}}\right) \qquad (10)$$

and

$$\ln (f(i_c, i_{\infty})) = \alpha a (-\eta) + \ln (i_o') \qquad (11)$$

where

$$f(i_c, i_{\infty}) = \frac{i_c e^{\frac{(\alpha f b i_{\infty})}{k'}}}{(1-\frac{b i_{\infty}}{k'})}$$

Thus, equation (10) tells us that i_{∞} will not be linearly related to $\sqrt{i_r}$ when $f>0$, meaning the discharge and recombination reactions are activated, probably due to a side reaction of H_2S with a hydrated electron, e^-_{aq} (10), as follows:

$$H_2S + e^-_{aq} \rightarrow H_2S^- \qquad (12)$$

and

$$H_2S^- + H^+ + M \rightarrow M\text{-}H + H_2S \qquad (13)$$

If $\ln(\frac{\sqrt{i_r}}{i_{\infty}})$ vs i_{∞} and $\ln(f(i_c i_{\infty}))$ vs η are linear, then this side reaction and overall mechanism can be said to be operating. Then, the coefficients k', k_3, α and i_o' can be computed from the slopes and intercepts of these plots, in conjunction with the iterative solution of equations (10) and (11). Eventually, θ_s vs η can be plotted; and θ_e, i_o and k_1 can be computed.

Once again, the potential ranges, where the recombination and discharge reactions are coupled, can be estimated from equations (7a) and (7b). With increasing H_2S concentration, these potential ranges have been found from analysis of available data according to the above model to become less negative, k_3 progressively decreases suggesting a decreasing surface diffusivity of H_{ad} atoms, and k_1

progressively increases suggesting that the discharge reaction is enhanced by the side reaction, equation (12), followed by equation (13). This will also explain why the overvoltage actually decreases rather than increases in the presence of H_2S.

Conclusions

A summary of a recently completed analysis of hydrogen electrode reactions during aqueous cathodic charging of metals is presented. The analysis for the first time takes into account the effect of hydrogen permeation into the metal on the h.e.r. From the model all of the kinetic parameters are computable without use of any adjustable parameters. For the first time, surface coverages and rate constants are determinable from the measured charging and permeation currents. The enhancement of hydrogen entry in the presence of poisons, such as H_2S, can be analyzed with the model, taking into account the Frumkin-Temkin isotherms in the discharge and recombination reaction kinetics.

Acknowledgment

Financial support by the Office of Naval Research under Contract No. NOOO14-84k-0201 is gratefully acknowledged.

References

1. M. Smialowski, Hydrogen in Steel, Pergamon Press, Oxford (1962).
2. C. M. Hudgins, Materials Protection, Vol. 8, p. 41 (1969).
3. J. O'M. Bockris, J. McBreen and L. Nanis, J. Electrochem. Soc., Vol. 112, p. 1025 (1965).
4. M. Zamanzadeh, A. Allam, H. W. Pickering and G. K. Hubler, J. Electrochem. Soc., Vol. 127, No. 8, p. 1688 (1980).
5. R. N. Iyer, M. Zamanzadeh and H. W. Pickering "Analysis of Hydrogen Evolution and Entry into Metals for the Coupled Discharge-Recombination Mechanism," (submitted to the J. Electrochemical Society).
6. C. D. Kim and B. E. Wilde, J. Electrochem. Soc., Vol. 118, p. 202 (1971).
7. B. E. Wilde and C. D. Kim, Corrosion, Vol. 42, No. 4, p. 243 (1986).
8. E. G. Dafft, K. Bohnenkamp and H. J. Engell, Corrosion Science, Vol. 19, p. 591 (1979).
9. E. Gileadi and B. E. Conway, Modern Aspects of Electrochemistry, No. 3, J. O'M. Bockris and B. E. Conway eds., Butterworths, Washington (1964), pp. 347-442.
10. R. N. Iyer, I. Takeuchi, M. Zamanzadeh and H. W. Pickering, "Hydrogen Sulfide Effect on Hydrogen Entry in Iron - A Mechanistic Study" (to be submitted to Corrosion).

BASIC DISTRIBUTION LIST

Technical and Summary Reports 1988

Organization	Copies
Defense Documentation Center Camerson Station Alexandria, VA 22314	12
Office of Naval Research Dept. of the Navy 800 N. Quincy Street Arlington, VA 22217 Attn: Code 1131	3
Naval Research Laboratory Washington, DC 20375 ATTN: Codes 6000 6300 2627	
Naval Air Development Center Code 606 Warminister, PA 18974 ATTN: Dr. J. DeLuccia	
Commanding Officer Naval Surface Weapons Center White Oak Laboratory Silver Spring, MD 20910 ATTN: Library	1
Naval Oceans Systems Center San Diego, CA 92132 ATTN: Library	1
Naval Postgraduate School Monterey, CA 93940 ATTN: Mechanical Engineering Department	1
Naval Air Systems Command Washington, DC 20360 Attn: Code 310A Code 5304B Code 931A	1 1 1
Naval Sea System Command Washington, DC 20362 ATTN: Code 05M Code 05R	1 1
Naval Air Prop. Test Ctr. Trenton, NY 08628 ATTN: Library	1
Naval Contruction Battallion Civil Engineering Laboratory Port Hueneme, CA 93043 ATTN: Materials Div.	1
Naval Electronics Laboratory San Diego, CA 92152 ATTN: Electron Materials Sciences Division	1
Naval Missile Center Materials Consultant Code 3312-1 Point Mugu, CA 92041	1
Commander David Taylor Research Center Bethesda, MD 20084	1
Naval Underwater System Ctr. Newport, RI 02840 ATTN: Library	1
Naval Weapons Center China Lake, CA 93555 ATTN: Library	1
NASA Lewis Research Center 21000 Brookpark Road Cleveland, OH 44135 ATTN: Library	1
National Bureau of Standards Gaithersburg, MD 20899 Attn: Metallurgy Division Ceramics Division Fracture & Deformation Division	1 1 1

Naval Facilities Engineering Command
Alexandria, VA 22331
ATTN: Code 03 1

Scientific Advisor
Commandant of the Marine Corps
Washington, DC 20380
ATTN: Code AX 1

Army Research Office
P.O. Box 12211
Research Triangle Park, NC 27709
ATTN: Metallurgy & Ceramics Program 1

Army Materials and Mechanics Research Center
Watertown, MA 02172
ATTN: Research Programs Office 1

Air Force Office of Scientific Research/NE
Building 410
Bolling Air Force Base
Washington, DC 20332
ATTN: Electronics & Materials Science Directorate 1

NASA Headquarters
Washington, DC 20546
Attn: Code RM 1

Defense Metals & Ceramics Information Center
Battelle Memorial Inst.
505 King Avenue
Columbus, OH 43201 1

Metals and Ceramics Div.
Oak Ridge National Laboratory
P.O. Box X
Oak Ridge, TN 37380 1

Los Alamos Scientific Lab.
P.O. Box 1663
Los Alamos, NM 87544
ATTN: Report Librarian 1

Argonne National Laboratory
Metallurgy Division
P.O. Box 229
Lemont, IL 60439 1

Brookhaven National Laboratory
Technical Information Division
Upton, Long Island
New York 11973
Attn: Research Library 1

Lawrence Radiation Lab.
Library
Building 50, Room 134
Berkely, CA 1

David Taylor Research Ctr
Annapolis, MD 21402-5067
ATTN: Code 281 1
Code 2813 1
Code 0115 1

RE/1131/88/75
4315 (036)

Supplemental Distribution List Feb 1988

Prof. I.M. Bernstein
Illinois Institute of Technology
IIT Center
Chicago, Ill 60615

Prof. H.K. Birnbaum
Dept. of Metallurgy & Mining Eng.
University of Illinois
Urbana, Ill 61801

Prof. H.W. Pickering
Dept. of Materials Science and Eng.
The Pennsylvania State University
University Park, PA 16802

Prof. D.J. Duquette
Dept. of Metallurgical Eng.
Rensselaer Polytechnic Inst.
Troy, NY 12181

Prof. J.P. Hirth
Dept. of Metallurgical Eng.
The Ohio State University
116 West 19th Avenue
Columbus, OH 43210-1179

Prof. H. Leidheiser, Jr.
Center for Coatings and Surface Research
Sinclair Laboratory, Bld. No. 7
Lehigh University
Bethlehem, PA 18015

Dr. M. Kendig
Rockwell International Science Center
1049 Camino Dos Rios
P.O. Box 1085
Thousand Oaks, CA 91360

Prof. R. A. Rapp
Dept. of Metallurgical Eng.
The Ohio State University
116 West 19th Avenue
Columbus, OH 43210-1179

Profs. G.H. Meier and F.S.Pettit
Dept. of Metallurgical and
Materials Eng.
University of Pittsburgh
Pittsburgh, PA 15261

Dr. W. C. Moshier
Martin Marietta Laboratories
1450 South Rolling Rd.
Baltimore, MD 21227-3898

Prof. P.J. Moran
Dept. of Materials Science & Eng.
The Johns Hopkins University
Baltimore, MD 21218

Prof. J. Kruger
Dept. of Materials Science & Eng.
The Johns Hopkins University
Baltimore, MD 21218

Prof. R.P. Wei
Dept. of Mechanical Engineering
and Mechanics
Lehigh University
Bethlehem, PA 18015

Prof. W.H. Hartt
Department of Ocean Engineering
Florida Atlantic University
Boca Raton, Florida 33431

Dr. B.G. Pound
SRI International
333 Ravenswood Ave.
Menlo Park, CA 94025

Prof. C.R. Clayton
Department of Materials Science
& Engineering
State University of New York
Stony Brook
Long Island, New York 11794

Prof. Boris D. Cahan
Dept. of Chemistry
Case Western Reserve Univ.
Cleveland, Ohio 44106

Dr. K. Sadananda
Code 6323
Naval Research Laboratory
Washington, D.C. 20375

Prof. M.E. Orazem
Dept. of Chemical Engineering
University of Virginia
Charlottesville, VA 22901

Dr. G.R. Yoder
Code 6384
Naval Research Laboratory
Washington, D.C. 20375

Dr. N. S. Bornstein
United Technologies Research Center
East Hartford, CT 06108

Dr. A.L. Moran
Code 2812
David Taylor Research Center
Annapolis, MD 21402-5067

Dr. B.E. Wilde
Dept. of Metallurgical Engineering
The Ohio State University
116 West 19th Avenue
Columbus, OH 43210-1179

Prof. G.R. St. Pierre
Dept. of Metallurgical Eng.
The Ohio State University
116 West 19th Avenue
Columbus, OH 43210-1179

Prof. G. Simkovich
Dept. of Materials Science & Eng.
The Pennsylvania State University
University Park, PA 16802

Dr. E. McCafferty
Code 6322
Naval Research Laboratory
Washington, D. C. 20375

Dr. J.A. Sprague
Code 4672
Naval Research Laboratory
Washington, D.C. 20375

Dr. C.M. Gilmore
The George Washington University
School of Engineering & Applied Science
Washington, D.C. 20052

Dr. F.B. Mansfeld
Dept. of Materials Science
University of Southern California
University Park
Los Angeles, CA 90089

Dr. Ulrich Stimming
Dept. of Chemical Eng. & Applied Chemistry
Columbia University
New York, N.Y. 10027

Prof. J. O'M. Bockris
Dept. of Chemistry
Texas A & M University
College Station, TX 77843